$M(C_6H_{16}N_3)_2(VO_3)_4$ as heterogeneous catalysts. Study of three new hybrid vanadates of cobalt(II), nickel(II) and copper(II) with 1-(2-aminoethyl)piperazonium.

Edurne S. Larrea[a], José L. Mesa[b], José L. Pizarro[a], Marta Iglesias[c], Teófilo Rojo[b] and María I. Arriortua*[a]

Received (in XXX, XXX) Xth XXXXXXXXX 20XX, Accepted Xth XXXXXXXXX 20XX
DOI: 10.1039/b000000x

Three new hybrid vanadates have been synthesized under hydrothermal conditions with the formula $M(C_6H_{16}N_3)_2(VO_3)_4$, where M= Co(II), Ni(II) and Cu(II). The structural analyses show that the phases are isostructural and crystallize in the monoclinic space group $P2_1/c$. These compounds show a two-dimensional crystal structure, with sheets composed of $[VO_3]_n^{n-}$ chains and metal centres octahedrically coordinated, chelated by two 1(2-aminoethyl)pyperazonium ligands. The thermal study reveals that copper containing phase is less stable than cobalt and nickel containing ones. The IR spectra of the three phases are very similar, with little differences in the inorganic bond region of the copper containing phase. The UV-visible spectra show that the cobalt(II) and the nickel(II) are in slightly distorted octahedral environments. The catalytic tests show that the phases act as heterogeneous catalysts for the selective oxidization of alkyl aryl sulfides, with both H_2O_2 and tert-butylhydroperoxide as oxidizing agents. The influence of the steric hindrance in the kinetic profile had been studied. The catalytic reactions induce the partial amorphization of the phases.

Introduction

Vanadium is one of the most interesting and reactive elements with a very rich chemistry in all of its oxidation states from +5 to -1. Its good catalytic activity, as well as its interesting sorption, optical, electrochemical and magnetic properties, are well documented in the literature[1]. Since the discovery of vanadate-dependent enzymes from various algae[2] and terrestrial fungi[3], the coordination chemistry of this element has received increasing interest.

Hybrid vanadates with first-row transition metals exhibit very rich crystal chemistry, with several structural archetypes according to the metal centre, the geometry of the ligand and the vanadium oxide subunit[4]. Each oxidation state of vanadium show different coordination environments. These polyhedra, range from the ideal octahedron, for the oxidation state three, to the tetrahedron, for the oxidation state five, going through the distorted octahedron, the square-based pyramid and the trigonal bipyramid (oxidation states four and five)[5]. In addition, vanadium polyhedra have a great ability to polymerize, giving rise to clusters, rings, chains, layers and three-dimensional frameworks[6]. The polymer grade is closely related to the synthetic conditions and, in particular, to the pH during the reaction[7].

The choice of the organic ligand is determinant for the structure of the resulting vanadates. Depending on the number of donor atoms, their relating positions to each other and the flexibility of the ligand, it could act chelating a metal centre or bridging two metal atoms. This fact, conditions the structure and, hence, the properties of the material.

In order to obtain open frameworks, there are two possible synthetic strategies. First, using long and rigid bridging ligands such as 4,4'-bypiridine, 1,2-bis(4-pyridil)ethylene or 1,2-bis(4-pyridil)ethane, which could act as pillars between inorganic sheets[8]. The other strategy comprises the use of chelating ligands, such as ethylenediamine, N,N'-*bis*(3-aminopropyl)ethylenediamine, *tris*(2-aminoethyl)amine, 2,2'-bipyridine, 1,10-phenantroline, etc., combined with low dimensionality vanadate subunits[9].

The last strategy was used to synthesize the vanadates included in this work, which were tested as heterogeneous catalysts for the oxidation of alkyl aryl sulfides. Sulfoxide derivatives are known to have interesting and useful biological and pharmacodynamic properties[10]. The sulfoxides are obtained by oxidation of thioethers by peracids, peroxides and alkyl peroxides using transition metal catalysts[11]. Depending on the catalyst selectivity and the method used, different proportions of sulfoxide and sulfone are produced[12].

Heterogeneous catalysis is a vital component of the chemical industry and it is involved to some degree in 90% of the chemical manufacturing processes currently in use[13]. On the other hand, catalytic oxidation in the liquid phase is becoming increasingly important in the synthesis of fine chemicals, where traditional processes employing stoichiometric inorganic oxidants are under increasing environmental pressure[14]. Catalytic oxidations in the liquid phase generally use soluble metal salts or complexes in

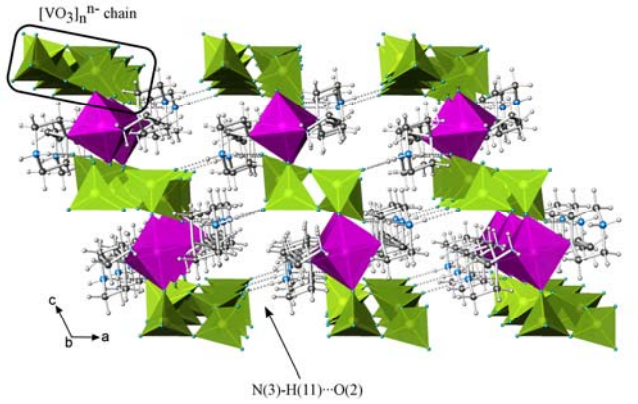

Fig. 1 Polyhedral view of the two-dimensional crystal structure.

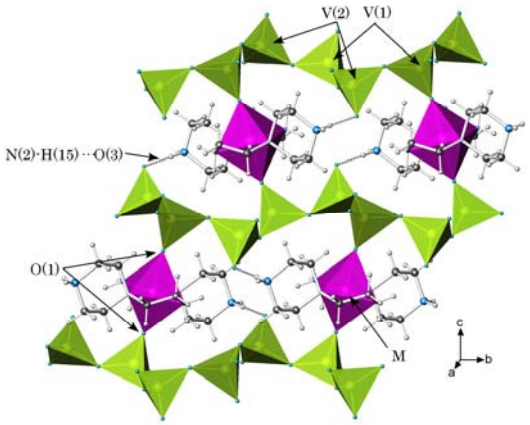

Fig. 2 Polyhedral view of (100) sheet.

combination with clean, inexpensive oxidants such as O_2, H_2O_2, or RO_2H. However, heterogeneous catalysts have the advantage of facile recovering and recycling.

As far as we are concerned, this is the first of catalytic properties of hybrid vanadates. There are some studies of related materials, such as vanadyl arsenates templated with amine molecules[15] or vanadyl phosphates[16], as well as of vanadium containing metal-organic compounds[17]. Recently, four silver(I) vanadates have also been studied as photocatalysts[18]. These compounds show a synergistic effect between silver ions and vanadate oxoanion that could improve their catalytic selectivity. All of them decompose methylene blue, a organic dye, under ultraviolet and/or visible light.

During the course of our study, in order to obtain new hybrid vanadates with catalytic properties, we have synthesized three new vanadates of Co(II), Ni(II) and Cu(II) with 1(2-aminethyl)pyperazonium (HAep+), with formula $M(HAep)_2(VO_3)_4$. In this work we report on the crystal structure, thermal behaviour, and spectroscopic properties together with the catalytic activity tests of these phases.

Results and discussion

Crystal structures

The structural analyses show that $Co(HAep)_3(VO_3)_4$, **1**, $Ni(HAep)_3(VO_3)_4$, **2** and $Cu(HAep)_3(VO_3)_4$, **3**, are isostructural and crystallize in the monoclinic space group $P2_1/c$, with very similar cell parameters. These compounds show a two-dimensional crystal structure (Fig. 1).

Vanadium(V) atoms are in tetrahedric coordination environments. Each VO_4 tetrahedra is linked to other two tetrahedra through two of their vertex. This joint, gives rise to $[VO_3]_n^{n-}$ chains in the [010] direction. On the other hand, the metallic ions, Co^{2+}, Ni^{2+} or Cu^{2+}, are octahedrally coordinated, linked to two O(1) atoms of two $[VO_3]_n^{n-}$ chains in the axial positions and to four nitrogen atoms of two $HAep^+$ molecules, in the equatorial plane. The organic molecule is chelating the metal centres *via* the nitrogen 1 of the pyperazine ring and the nitrogen of the aminoethylic radical. The other nitrogen atom of the ring is protonated.

The joint between the octahedra and the vanadate chains through the O(1) atoms gives rise to the sheets, parallel to the (100) plane (Figure 2). These sheets are linked to each other *via* hydrogen bonds between the hydrogen atom H(11), bonded to the protonated nitrogen atom, N(3), of the $HAep^+$, and the O(2) atom of the $[VO_3]_n^{n-}$ chain, N(3)-H(11)···O(2) (Figure 1). There are, also, hydrogen bonds into the (100) sheets.

The M-N distances are very similar for the three compounds and range from 1.992(1) to 2.271(1) Å. However, the M-O distances of phase **3** are higher than those of the phases **1** and **2**. For the cobalt(II) and nickel(II) compounds, the M-O distances are approximately 2.1 Å, whereas for the copper(II) phase, this distance is of 2.330(1) Å. This difference is due to the Jahn-Teller effect of the Cu(II) cation, whose octahedra are slightly elongated, and, as a consequence, the c parameter of the phase **3** is unexpectedly bigger than that of the nickel(II) containing one. The *cis* angles range from 81.82(5) º to 98.18(5) º and the *trans* ones are 180 º, because the metallic atoms are at special positions, over symmetry centres.

The V-O bond distances observed in the vanadium(V) tetrahedra are in the normal range for this oxoanion[19]. Depending on the connectivity of the oxygen atom the V-O distances can be classified as short (approx. 1.6 Å), when the oxygen is terminal, as medium (1.65-1.70 Å), when the oxygen is linked to the metal, or as long (approx. 1.8 Å), when the oxygen is linked to another vanadium atom. In this structure, there are two crystallographically independent vanadium(V) atoms, with three terminal oxygen bonds, one oxygen shared with a divalent metal and two shared by two vanadium(V) atoms. However, only one short distance, of 1.62 Å, is found, for the V(2)-O(6) bond. The other two terminal oxygen atoms, O(2) and O(3), have distance near 1.65 Å, because they are part of hydrogen bonds. The medium bond distances are formed by V(1)-O(1), and are of 1.657(1) and 1.658(1) Å for phases **1** and **2**, whereas for phase **3** is 1.631(1) Å, smallest than expected. This fact is related with the Jahn-Teller effect mentioned above: the O(1) is more distant from the copper(II) atom, and, therefore, in the tetrahedra takes a medium distance between the terminal oxygen atom and the oxygen atom shared with a metallic centre. The bond distances V-O(4) and V-O(5), where the oxygen atoms are shared between both crystallographicaly independent vanadium(V) atoms, are around 1.8 Å, as expected. The bond angles of the vanadium(V) tetrahedra range from 107.4(1) to 112.3(1) º. Bond distances of the described polyhedra are included in Table 1.

To complete the structural description, the polyhedral distortion study was carried out by the Continuous Symmetry Measure

Table 1 *Selected bond distances (Å) for **1, 2** and **3**.*

V(1)O4 tetrahedra			
	1	2	3
V(1)-O(2)	1.648(1)	1.653(1)	1.653(1)
V(1)-O(1)	1.657(1)	1.658(1)	1.631(1)
V(1)-O(5)	1.776(1)	1.785(1)	1.787(1)
V(1)-O(4)	1.781(1)	1.781(1)	1.784(1)

$V(2)O_4$ tetrahedra			
	1	2	3
V(2)-O(6)	1.648(1)	1.629(1)	1.624(1)
V(2)-O(3)	1.657(1)	1.651(1)	1.652(1)
V(2)-O(5)	1.776(1)	1.807(1)	1.804(1)
V(2)-O(4)^{ii}	1.781(1)	1.811(1)	1.807(1)

MO_2N_4 octahedra			
	1	2	3
M-O(1)^{i}	2.104(1)	2.093(1)	2.330(1)
M-O(1)	2.104(1)	2.093(1)	2.330(1)
M-N(2)^{i}	2.119(1)	2.075(1)	1.992(1)
M-N(2)	2.119(1)	2.075(1)	1.992(1)
M-N(1)^{i}	2.271(1)	2.227(1)	2.182(1)
M-N(1)	2.271(1)	2.227(1)	2.182(1)

$(C_6H_{16}N_3)$ 1-(2-aminoethyl)-piperazonium			
	1	2	3
N(2)-C(2)	1.474(2)	1.479(2)	1.478(2)
C(2)-C(6)^{i}	1.502(3)	1.502(2)	1.504(2)
N(1)-C(6)	1.495(2)	1.499(2)	1.499(2)
N(1)-C(1)	1.482(2)	1.477 (2)	1.484(2)
N(1)-C(4)	1.482(2)	1.493(2)	1.487(2)
N(3)-C(3)	1.485(2)	1.489(2)	1.476(2)
N(3)-C(5)	1.490(2)	1.4929(2)	1.477(2)
C(1)-C(5)	1.516(2)	1.525(2)	1.519(2)
C(3-C(4)	1.517(2)	1.523(2)	1.519(2)

Symmetry codes:

i= -x, -y, -z ii= -x, y+1/2, -z+1/2

a

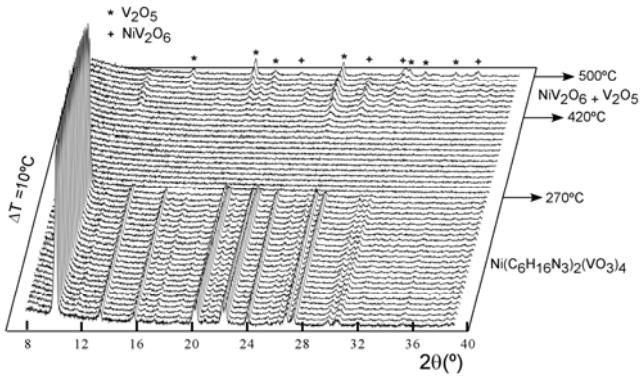

Fig. 3 Thermodiffractogram of compound **2**.

(CSM)[20], method based on the comparison between the real polyhedron and the most similar ideal one. These calculations were carried out with the Shape v1.1a program, developed by S. Alvarez *et al*[21]. The S(Oh) values for phases **1**, **2** and **3** are 0.49, 0.34 and 0.59, respectively, which represent very slight distortions with regard to the ideal octahedron[22]. The S(Td) values calculated for the vanadium(V) tetrahedra are around 0.12 for V(1) and 0.25 for V(2). This values indicate that the vanadium(V) environment is very regular[23].

Thermal Study

The thermogravimetric decomposition curves of the three phases show a sequence of overlapped processes of mass loss, from approximately 250 ºC to almost 500 ºC for compounds **1** and **2**. Whereas, for compound **3**, these processes occur between 185 and 470 ºC. The total weight loss is 38.9 % for **1**, 38.8 % for **2** and 38.1 % for **3**. These mass percentages are very close to the theoretic percentages of the organic cation into the phases, 37.2, 37.3 and 36.2 %, respectively. The excess of mass that gets lost during the heating process could correspond to the evaporation of the sample at high temperature. The calcination products were identified by X-ray powder diffraction analysis. The residue of **1** consists of $Co_2V_2O_7$ [$P2_1/c$, a=6.599 Å, b= 8.388 Å, c= 9.492 Å, β= 100.17 º][24] and V_2O_5 [$Pmn2_1$, a= 11.503 Å, b=4.369 Å, c= 3.557 Å][25]. The residue of **2** consist of a mixture of NiV_3O_8 [a= 13.310 Å, b= 8.395 Å, c= 10.040 Å][26], and V_2O_5[25]. Finally, the copper(II) phase, **3**, decomposed in $Cu_2V_2O_7$ [C2/c, a= 7.687 Å, b= 8.007 Å, c= 10.090 Å, β= 1140.45 º][27] and V_2O_5[25].

The thermal behaviour of the phases was also studied using time-resolved X-ray diffractometry (Fig. 3). Phases **1** and **2** are stable until 270 ºC and 280 ºC, respectively. The copper(II) phase is less stable, and its structure collapses at 180 ºC. The destruction of the crystal structure is due to the calcination of the organic ligand, according to the thermogravimetric data. Above these temperatures, the formation of amorphous compounds takes place. In the case of phase **1**, the heating residues crystallise at 380 ºC, for phase **2** the diffraction maxima start to appear at 430 ºC, and in the case of **3**, this crystallization process occurs at 360 ºC. At the end of the heating process two phases were determined for the cobalt(II) compound: $Co_2V_2O_7$[24] and V_2O_5[25]. For phase **2** a mixture of $Ni_2V_2O_7$ [$P2_1/c$, a=6.515 Å, b= 8.303 Å, c= 9.350 Å, β= 99.86 º][28] and V_2O_5[25] is obtained. The thermal decomposition of **3** gives rise to a mixture of CuV_2O_6 [P-1, a= 9.170 Å, b= 3.552

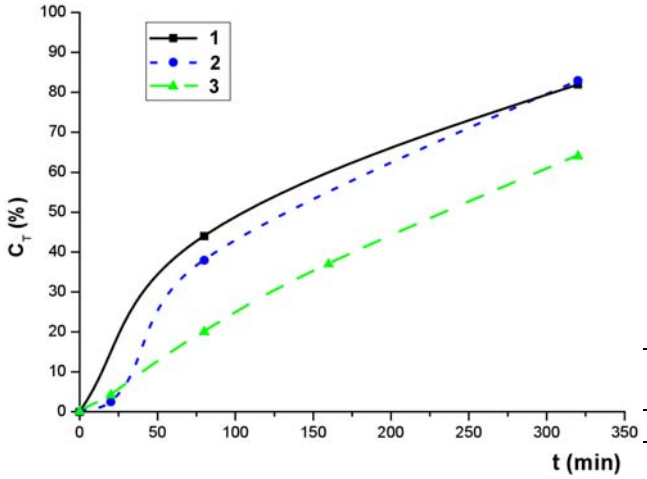

Fig. 4 Kinetic profiles of **1**, **2** and **3** for the oxidation reaction of methyl phenyl sulfide.

Å, c= 6.480 Å, α= 92.30 º, β= 110.35 º, γ= 91.78 º][29] and V_2O_5[25]. In the thermal stability range of the phases, an angular variation on the diffraction maxima can be observed, due to the thermal expansion of the unit cell parameters. Thermodiffractometry of phase **2** is shown on Figure 3 as an example.

The temperature at which the crystal structure of **3** collapses is significantly lower, comparing with the isostructural phases. This lower stability temperature is due to the weaker bonds that Cu^{2+} establishes with the O(1), doing the framework less stable.

IR and UV-Visible (diffuse reflectance) spectroscopy

In the IR spectra of the three phases there are two characteristic regions, the first one, between 3300 and 990 cm^{-1}, where the bands due to the vibration of the organic molecule bonds appeared, and the later one, between 950 and 500 cm^{-1}, where the vibrations of the vanadate groups are detected. The three spectra are very similar (Fig. 5). Only the spectrum of **3** has some differences, mainly in the inorganic bond region, due to the differences observed in the Cu-O bond distances.

The UV-visible spectra of phases **1** and **2** show that the cobalt(II) and the nickel(II) are in a slightly distorted octahedral environment. Taking into account the absorption band positions it was possible to calculate the crystal field splitting parameter, Dq, and the Racah parameters, B and C for **1**, and only B for **2**. For **1**, Dq= 935 cm^{-1}, B= 710 cm^{-1}, 65 % of the free ion ($B_o(Co^{2+})$= 1115 cm^{-1})[30] and C= 4765 cm^{-1}. For **2**, Dq= 1100 cm^{-1} and B= 630 cm^{-1}, approximately 60 % of the free ion ($B_o(Ni^{2+})$= 1030 cm^{-1})[31]. In the case of **3** it is not possible to calculate these parameters, because of the electronic configuration of the copper(II) ion, d^9, and the tetragonal distortion shown by the coordination polyhedron in this structure. The bands of this spectrum are due to d-d transitions between components of the same ionic term[32].

Catalytic Activity

Vanadium peroxides are known as very effective oxidants of different organic and inorganic substrates such as sulfides, alkenes, alcohols, aromatic and aliphatic hydrocarbons, halides and sulfur dioxide[33]. These reactions, either stoichiometric or catalytic, where the terminal oxidant is normally hydrogen peroxide or an alkylhydroperoxide, are carried out, on average, in

Table 2 *Conversion (C_T), selectivity towards the sulfoxides formation (S_{SO}) and turnover frequency (TOF) data of oxidation of alkyl aryl sulfides catalyzed by **1**, **2** and **3**.*

Catalyst	Substrate	Oxidizing Agent	C_T(%) (t, min)	S_{SO} (%)	TOF (min^{-1})
1	MeSPh	H_2O_2	82 (320)	95	0.54
	MeSPh	TBHP	89 (370)	90	1.40
2	MeSPh	H_2O_2	83 (320)	94	0.48
3	MeSPh	H_2O_2	64 (320)	95	0.26
	EtBuSPh	H_2O_2	93 (380)	90	0.44
	MeSClPh	H_2O_2	99 (320)	84	1.01
	MeS*p*-tolyl	H_2O_2	100 (380)	96	1.37

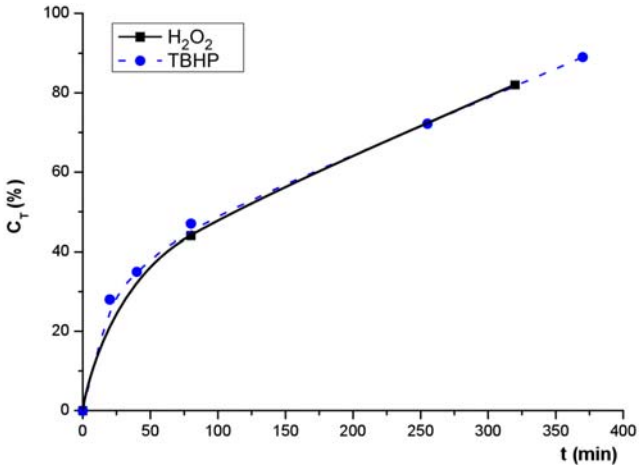

Fig. 5 Kinetic profiles of the oxidation reaction of methyl phenyl sulfide with H_2O_2 and TBHP as oxidizing agents over catalyst **1**.

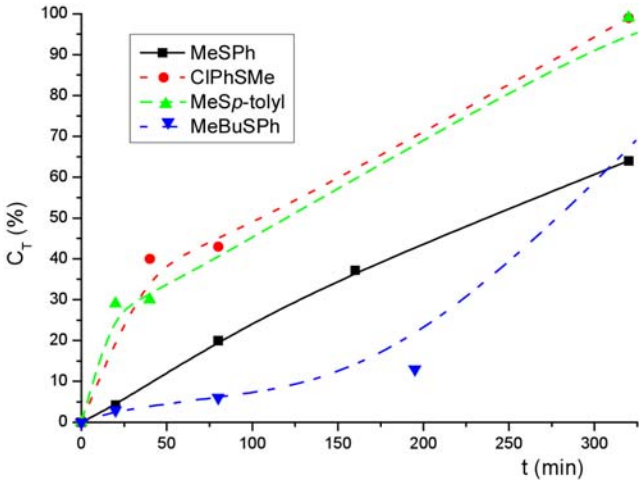

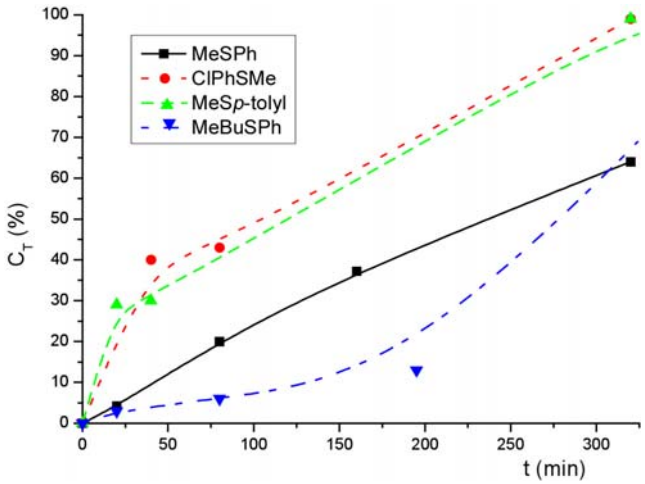

Fig. 6 Kinetic profiles of the oxidation reaction of methyl phenyl sulfide (MeSPh), 4-chlorophenyl methyl sulfide (4-ClPhSMe), methyl *p*-tolyl sulfide (MeS*p*-tolyl) and ethylbuthyl phenyl sulfide (EtBuSPh) over the catalyst **3** with H_2O_2 as oxidizing agent.

mild conditions and associated to good product yield and selectivity.

The activity of the vanadium catalysts **1**, **2** and **3**, was probed towards oxidation of sulfides. To note, this reaction is interesting both for the preparation of sulfoxides and sulfones[33], as well as for desulfurization of fuels[34].Various catalytic essays were performed with different oxidizing agents (H_2O_2 and TBHP) and substrates (methyl phenyl sulfide, ethylbutyl phenyl sulfide, *p*-chlorophenyl methyl sulfide and methyl *p*-tolyl sulfide) (Table 2). First of all, the catalysts were tested for the oxidation of methyl phenyl sulfide with H_2O_2 as oxidizing agent. In figure 4 the kinetic profiles of these reactions are shown. The behaviour of all the catalysts is very similar, reaching conversions between 83 and 64 %, with selectivity rates towards the sulfoxide over 94 %.

The influence of the oxidizing agent was studied comparing the kinetic profiles of the oxidation reactions of methyl phenyl sulfide with H_2O_2 and TBHP over catalyst **1** (Fig. 5). The profiles are very similar to each other, observing no loss in the conversion rate when increasing the steric hindrance of the oxidizing agent.

On the other hand, when the steric hindrance of the substrate is increased the kinetic profile and the conversion and selectivity rates change (Fig. 6). The reactions were made over the catalyst **3**, using H_2O_2 as oxidizing agent, and with the substrates ethylbutyl phenyl sulfide, *p*-chlorophenyl methyl sulfide and methyl *p*-tolyl sulfide. In figure 6 the kinetic profiles of these reactions are shown. When a substituent is introduced in the phenyl ring of the substrate (Cl, Me), an increase in the TOF and conversion rate is observed. However, the kinetic profile for ethylbutyl phenyl sulfide shows an important induction period due to steric hindrance presented by this substrate, which makes the access to the active site more difficult.

When the reactions are completed, the catalysts were filtered, washed, dried and characterized by powder X-ray diffraction and IR spectroscopy. When the catalysts are used for the oxidation of methyl phenyl sulfide with H_2O_2, the diffraction patterns show the diffraction maxima of the corresponding crystal structure, but the background is significantly higher, due to the amorphization of the material during the reaction (Fig. 7). However, when

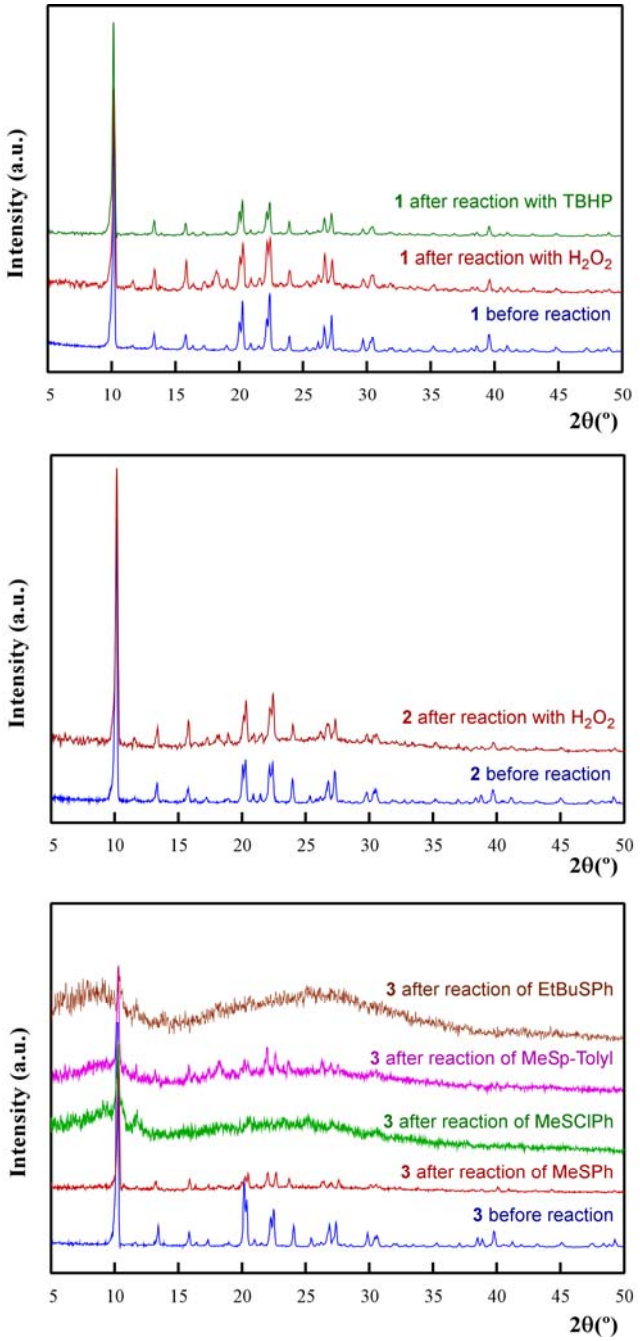

Fig. 7 Powder diffraction patterns of the catalysts before and after the reactions.

TBHP is used, the diffraction pattern of **1** does not show any amorphization. Finally, the oxidation reactions of ethylbutyl phenyl sulfide, *p*-chlorophenyl methyl sulfide and methyl *p*-tolyl sulfide produce an important amorphization of the catalysts, being observed almost only the first maxima of the diffraction pattern of **3**. The IR spectra of the catalysts **1**, **2** and **3**, before and after the reaction with methyl phenyl sulfide are almost equal. On the other hand, catalyst **3** after reacting with ethylbutyl phenyl sulfide, *p*-chlorophenyl methyl sulfide and methyl *p*-tolyl sulfide show IR spectra with very different features, although the bands due to the organic cation and V-O bonds appear. It is very likely that the amorphous phases obtained after the reactions keep the connectivity of the original phase to some extent, even though the

Table 3 Details of the crystal data, structural resolution and refinement procedure for **1, 2** and **3**.

Compound	**1**	**2**	**3**
Formula	$C_6H_{16}Co_{0.5}N_3O_6V_2$	$C_6H_{16}Ni_{0.5}N_3O_6V_2$	$C_6H_{16}Cu_{0.5}N_3O_6V_2$
Formula weight	357.56	357.45	359.86
Crystal system	Monoclinic	Monoclinic	Monoclinic
Space group (nº)	$P2_1/c$ (14)	$P2_1/c$ (14)	$P2_1/c$ (14)
a, Å	9.881(1)	9.848(1)	9.763(1)
b, Å	9.400(1)	9.442(1)	9.295(1)
c, Å	15.024(2)	14.965(1)	15.158(2)
β, º	116.54(1)	116.52(1)	116.31(1)
V, $Å^3$	1248.4(2)	1245.2(2)	1233.0(2)
Z	4	4	4
ρ_{obs}, ρ_{calc}, $gr{\cdot}cm^{-3}$	1.90(1), 1.902	1.90(1), 1.907	1.93(1), 1.939
F(000)	722	724	726
Temperature, K	293(2)	293(2)	293(2)
Diffractometer	Stoe IPDS	Stoe IPDS	O. D. Xcalibur2
Radiation, λ(Mo Kα), Å	0.71073	0.71073	0.71073
μ mm^{-1}	2.159	2.254	2.376
Crystal size, mm	0.17x0.17x0.05	0.28x0.25x0.15	0.25x0.20x0.05
θ range, º	2.87-29.78	3.60-33.14	2.87-32.62
Limiting indices, h, k, l	h=±13, k=±13, l±20	h=±15, -11≤k≤10 -19≤l≤22	-14≤h≤13, -12≤k≤13, -21≤l≤22
Nº reflections measured	24283	16043	12128
Nº reflections unique	3531	4583	4069
R(int)	0.0446	0.0314	0.0255
Data/Restrain/Param.	3531/0/160	4583/0/160	4069/0/161
Final R indices [I>2σ(I)]	R1= 0.0240, wR2= 0.0379	R1= 0.0245, wR2= 0.0484	R1= 0.0284 wR2= 0.0677
R indices [all data]	R1= 0.0412, wR2= 0.0396	R1= 0.0378, wR2= 0.0506	R1= 0.0393 wR2= 0.0709
w= $1/[\sigma^2\|F_o\|^2+(xp)^2]$, p=$[max\|F_o\|^2+2\|F_c\|^2]/3$	x= 0.015	x= 0.0273	x=0.0426
Largest diff. peak and hole, $e.Å^{-3}$	0.409, -0.235	0.411, -0.359	0.712,-0.438
G. O. F	0.944	0.921	0.990

[a] $R_1 = \sum \| |F_o| - |F_c| \| / \sum |F_o|$; $wR_2 = \sqrt{\sum w(|F_o| - |F_c|)^2 / \sum w|F_o|^2}$

order is not maintained.

Experimental

Synthesis and characterization

$Co(HAep)_3(VO_3)_4$, **1**, $Ni(HAep)_3(VO_3)_4$, **2** and $Cu(HAep)_3(VO_3)_4$, **3**, have been synthesized using mild solvothermal conditions employing PTFE (poly-tetrafluoroethylene) reactors. In a typical synthesis of **1**, a mixture of 250 mg (0.86 mmol) of $Co(NO_3)_2.6H_2O$, 157 mg (1.28 mmol) of $NaVO_3$, 225 μl (1.72 mmol) of 1-(2-aminoethyl)-piperazine (Aep) in 20 ml of methanol and 10 ml of distilled water, pH= 10, was heated at 120 ºC for three days. This gave a mixture of orange prismatic crystals of **1** and an unidentified yellow powder. Crystalline product was separated from the powder, washed with distilled water and acetone, and dried at ambient temperature.

The synthesis of **2** involved mixing 250 mg (0.86 mmol) of $Ni(NO_3)_2.6H_2O$, 104.82 mg (0.86 mmol) of $NaVO_3$, 225 μl (1.72 mmol) of Aep in 20 ml of 1-butanol and 10 ml of distilled water, giving a pH of 9. The reaction conditions were the same as those

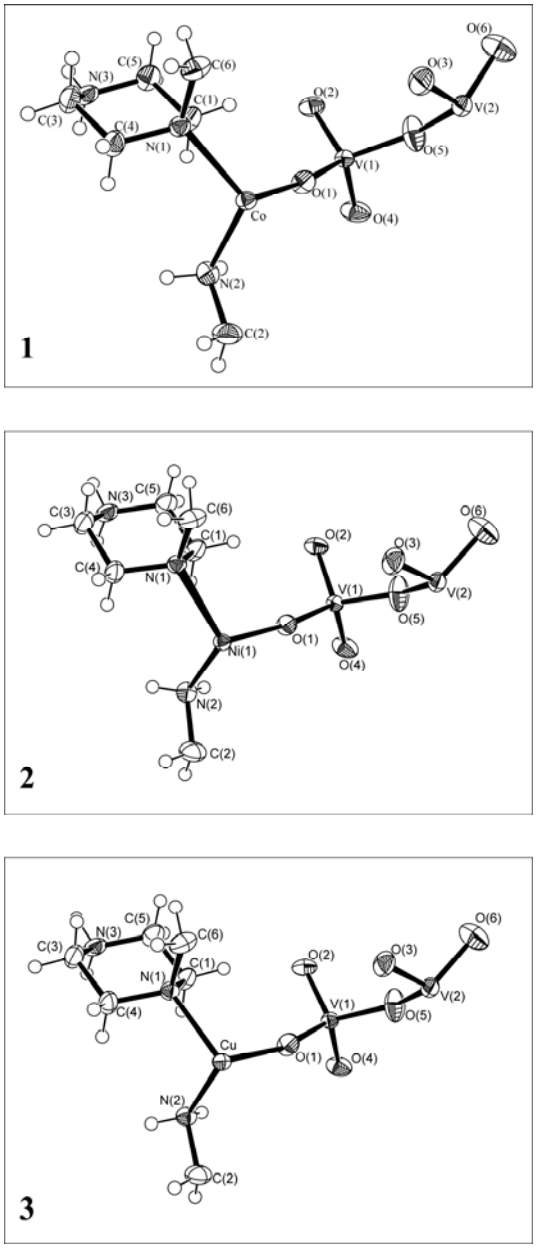

Fig. 8 Asymmetric unit and the atomic labelling scheme of phases **1**, **2** and **3.** Thermal ellipsoid plot (50 %).

used in the synthesis of **1**. After slow cooling to room temperature, green prismatic crystals appeared as the major product together with a small amount of an unidentified brown yellowish powder. Crystalline product was separated from the powder, washed with distilled water and acetone, and dried at ambient temperature.

In the synthesis of **3** 350.00 mg (1.5 mmol) of $Cu(NO_3).2.5H_2O$ salt was mixed with 227.50 mg (1.87 mmol) of $NaVO_3$ and 175 µl (1.3 mmol) of Aep in 20 ml of methanol an 10 ml of distilled water. The mixture, with a pH of 6, was heated up to 100 ºC for three days. After cooling the reaction system to room temperature, a mixture of light blue prismatic crystal and a brown greenish unidentified powder was obtained. The crystals were separated from the powder, washed with water and acetone and dried.

The amounts of cobalt, nickel, copper and vanadium in compounds **1, 2** and **3** were measured by inductively coupled plasma - atomic emission spectrometry and the amounts of C, N and H by elemental analysis. Calculated (%) for **1**: Co, 8.2; V, 28.5; C, 20.2; N, 11.8; H, 4.5. Found (%) Co, 8.5(1); V, 29.2(2); C, 20.0(1); N, 11.6(1); H, 4.4(1). Calculated (%) for **2**: Ni 8.2; V, 28.5; C, 20.2; N, 11.8; H, 4.5. Found (%) Ni, 8.8(1); V, 28.8(2); C, 19.9(1); N, 11.7(1); H, 4.5(1). Calculated (%) for **3**: Cu 8.8; V, 28.3; C, 20.0; N, 11.7; H, 4.5. Found (%) Cu, 10.2(1); V, 27.4(2); C, 19.9(3); N, 11.4(1); H, 4.5(1). The densities of the three phases were measured by flotation method[35], using a mixture of CH_2I_2 and CH_2Cl_2, being 1.90(1) g/cm^3 for **1**, 1.90(1) g/cm^3 for **2** and 1.93(1) g/cm^3 for **3**.

Single-crystal X-ray diffraction

Prismatic single crystals of compounds **1**, **2** and **3** with dimensions 0.17x0.17x0.05 mm, 0.28x0.25x0.15 mm and 0.29x0.20x0.05 mm, respectively, were carefully selected under a polarizing microscope and glued on a glass fibre. Diffraction data were collected on a Stoe IPSD XArea diffractometer for **1** and **2**, and on a Xcalibur2 diffractometer for **3,** using in all cases graphite monochromated Mo Kα radiation. Details of crystal data, intensity collection, and some features of the structural refinement are reported in Table 3.

The diffraction data were corrected for Lorentz and polarization effects[36]. Absorption effect[37] was also corrected by using the diffractometer software[38]. The structures were solved by direct methods (SHELXS 97)[39] and then refined by the full-matrix least-squares procedure based on F^2, using the SHELXL 97 computer program[39] belonging to the WINGX software package[40]. The scattering factors were taken from Ref 41. Anisotropic thermal parameters were assigned to the non H atoms (Fig. 8). The hydrogen atoms were generated geometrically. At convergence, R1= 0.0240, wR2= 0.0379 for **1**, R1= 0.0245, wR2=0.0484 for **2** and R1= 0.0284, wR2=0.0677 for **3**, with I> 2σ(I).

Physicochemical characterization techniques

The thermal analyses were carried out using a STD 2960 Simultaneous DSC-TGA TA Instruments thermobalance for phases **1** and **2**, and with a NETZSCH STA 449 C for phase **3**. A crucible containing approximately 10 mg of sample was heated at 5 °Cmin^{-1} in the temperature range 30-500 °C. The thermal behaviour was also studied using time-resolved X-ray diffractometry. A Bruker D8 Advance Vantec diffractometer (Cu Kα radiation) equipped with a variable-temperature stage (Anton Paar HTK2000) with a Pt sample holder was used in the experiments. The powder patterns were recorded in 2θ steps of 0.01667º in 8-45º range, counting for 0.1 s per step and increasing the temperature at 10 ºCmin^{-1} from room temperature to 450 °C, in the case of compound **1**, and to 500 ºC for compound **2** and **3**.

The IR spectra (KBr pellets) were obtained with a Nicolet FT-IR 740 spectrophotometer in the 4000-400 cm^{-1} range. The UV-visible spectra by diffuse reflectance of **1**, **2** and **3** powder samples were registered at room temperature on a Varian Cary 5000 spectrometer in the 200-1800 nm range.

Catalytic activity

Oxidation of organic sulfides was carried out in a batch reactor at

atmospheric pressure, using acetonitrile or dichloromethane as solvents (2 ml). Before the reactions the materials (0.007 mmol) were activated by stirring them with the oxidizing agent, H_2O_2 or *tert*-butyl hydroperoxide (TBHP) in the corresponding solvent, acetonitrile or dichloromethane, for 30 min at 70 ºC or 50 ºC, respectively. After this activation stage, the catalysts were separated from the liquid media. The reactor with the activated catalyst was then charged with 3 mmol of the corresponding sulfide (methyl phenyl sulfide, 4-clorophenyl methyl sulfide, methyl *p*-tolyl sulfide and 1-ethylbutyl phenyl sulfide) (ratio V/substrate= 1:100) in 2 ml of solvent. The oxidizing agent was added dropwise and then the suspension was heated to 70 ºC, when using H_2O_2, and to 50 ºC, with TBHP. Experiments in the same reaction conditions without catalyst have been also conducted and no appreciable amount of product was detected. Reaction samples were taken at regular times and analyzed by a Hewlett-Packard 5890 II GC-MS in order to determine the conversion. After the reaction, the catalysts were filtered and characterized by X-ray powder diffraction and IR spectroscopy.

Conclusions

We report the synthesis and characterization of three isostructural vanadates of cobalt(II), nickel(II) and copper(II) with the cationic ligand 1-(2-aminoethyl)piperazonium. These phases present a two-dimensional crystal structure in which the organic molecule is monoprotonated and linked to the metallic centres *via* nitrogen atoms. There are interlayer hydrogen bonds between the protonated amine and terminal oxygen atoms of the vanadate groups. The thermal stability of the phases depends on the metal that compose them, being the less stable the copper(II) containing one. The catalytic tests show that the phases are active and oxidize selectively alkyl aryl sulfides. The use of TBHP as oxidizing agent, instead of H_2O_2, does not actually affect to the kinetic profile of the reaction. However, the increase of steric hindrance in the alkyl substituent of the sulfide causes an important change in the kinetic profile, which has an activation stage not shown in the case of other sulfides. When the oxidizing agent is H_2O_2, the catalytic reactions induce the partial amorphization of the catalysts. Although the long-range order is lost after the reactions, the connectivity between the components of the phases is maintained.

Acknowledgements

This work has been financially supported by the "Ministerio de Ciencia e Innovación" (MAT2010-15375, MAT2006-14274-C02-02), the "Gobierno Vasco" (IT177-07), which we gratefully acknowledge. We also thank the technicians of SGIker (UPV/EHU), Drs. J. Sangüesa, I. Orue, A. Larrañaga, J.C. Raposo, L. Bartolomé and P. Vitoria, financed by the National Program for the Promotion of Human Resources within the National Plan of Scientific Research, Development and Innovation (Ministerio de Ciencia e Innovación) and the European Social Fund (ESF), for the X-ray diffraction and chemical, spectroscopic and magnetic measurements. Edurne S. Larrea thanks the UPV/EHU for funding.

Notes and references

[a] *Dpto. Mineralogía y Petrología, Universidad del País Vasco (UPV/EHU), Apdo. 644, 48080 Bilbao, Spain. Fax: 0034 946 013 500; Tel: 0034 946 012 534; E-mail: maribel.arriortua@ehu.es*
[b] *Dpto. Química Inorgánica, Universidad del País Vasco (UPV/EHU), Apdo. 644, 48080 Bilbao, Spain.*
[c] *Instituto de Ciencia de Materiales de Madrid, CSIC, c/ Sor Juana Inés de la Cruz 3, Cantoblanco, 28049, Madrid, Spain.*
† CCDC reference numbers 826549-826551.For crystallographic data see DOI: 10.1039/b000000x/

1 R.A. Shiels, K. Venkatasubbaiah, C.W. Jones, *Adv. Synth. Catal.*, 2008, **350**, 2823; A. Zhang, J. Zhang, N. Cui, X. Tie, Y. An, L. Li, *J. Mol. Catal. A-Chem.*, 2009, **304**, 28; D.E. Katsoulis, *Chem. Rev.*, 1998, **98**, 359; G. Centi, F. Trifiro, *Appl. Catal. A: General*, 1996, **143**, 3; Y. Idota, *Eur. Pat.*, 0 567 149 A1, 1993; M.S. Whittingham, *J. Electrochem. Soc.: Electrochem. Sci. Tech*, 1976, **123**, 315; S. Denis, E. Baudrin, F. Orsini, G. Ouvrard, M. Touboul, J.-M. Tarascon, *J. Power Sources*, 1999, **81-82**, 79; Y. Ueda, *Chem. Mater.*, 1998, **10**, 2653; L. Liu, X. Wang, A.J. Jacobson, *J. Mat. Res.*, 2009, **24**, 1901.
2 M. Weyad, H.J. Hecht, M. Kiess, M.F. Liaud, H. Vilter, D. Schomburg, *J. Mol. Biol.*, 1999, **293**, 595; J.N. Carter-Franklin, J.D. Parrish, R.A. Tchirret-Guth, R.D. Little, A. Butler, *J. Am. Chem. Soc.*, 2003, **125**, 3688; D. Rechder, G. Santoni, G.M. Licini, C. Schilzke, B. Meier, *Coord. Chem. Rev.*, 2003, **237**, 53.
3 A. Butler, *Coord. Chem. Rev.*, 1999, **187**, 17.
4 R. Fernández de Luis, M.K. Urtiaga, J.L. Mesa, T. Rojo, M.I. Arriortua, *J. Alloys Comp.*, 2009, **480**, 54.
5 M. Schindler, F.C. Hawthorne, W.H. Baur, *Chem. Mater.*, 2000, **12**, 1248.
6 P. Y. Zavalij, M. S. Whittingham, *Acta Crystallogr., Sect. B*, 1999, **55**, 627.
7 M. Schindler, F. C. Hawthorne, W. H. Baur, *Can. Mineral.*, 2000, **38**, 1443; J. Livage, *Coord. Chem. Rev.*, 1998, **178–180**, 999.
8 R. Fernández de Luis, J.L. Mesa, M.K. Urtiaga, L. Lezama, M.I. Arriortua, T. Rojo, *New J. Chem.*, 2008, **32**, 1; R. Fernández de Luis, M.K. Urtiaga, J.L. Mesa, K. Vidal, L. Lezama, T. Rojo, M.I. Arriortua, *Chem. Mater.*, 2010, **22**, 5543.
9 E.S. Larrea, J.L. Mesa, J.L. Pizarro, J. Rodríguez-Fernández, M.I. Arriortua, T. Rojo, *Eur. J. Inorg. Chem.*, 2009, 3607; J. Do, A.J. Jacobson, *Inorg. Chem.*, 2001, **40**, 2468; P.J. Hagrman, J. Zubieta, *Inorg. Chem.*, 2001, **40**, 2800.
10 A.G. Renwick, in, *Sulfur-Containing Drugs and Related Organic Compounds*, ed. L.A. Damani, Horwood, Chichester, 1989, vol. 1, part B, p. 133.
11 F. Bonadies, F. De Angelis, L. Locat, A. Scettri, *Tetrahedron Lett.*, 1996, **37**, 7129.
12 D. Alonso, C. Nájera, M. Varea, *Tetrahedron Lett.*, 2002, **43**, 3459.
13 P.M. Forster, A. K. Cheethanm, *Top. Catal*., 2003, **24**, 79.
14 R.A. Sheldon, R.S. Downing, *Appl. Catal. A*, 1999, **189**, 163.
15 T. Berrocal, J.L. Mesa, J.L. Pizarro, B. Bazan, M. Iglesias, A.T. Aguayo, M.I. Arriortua, T. Rojo, *Chem. Commun.*, 2008, **39**, 4738; T. Berrocal, J.L. Mesa, J.L. Pizarro, B. Bazan, M. Iglesias, J.L. Vilas, T. Rojo, M.I. Arriortua, *Dalton Trans.*, 2010, **39(3)**, 834; T. Berrocal, E.S. Larrea, M. Iglesias, M.I. Arriortua, *J. Mol. Cat. A: Chem.*, 2011, **335(1-2)**, 176.
16 P. Amorós, D. Marcos, A. Beltrán-Porter, *Curr. Opin. Solid State Mater. Sci.*, 1999, **4**, 123; H. Imai, Y. Kamiya, T. Okuhara, *J. Catal.*, 2008, **255**, 213; Y.H. Taufiq-Yap, A.A. Rownaghi, M.Z. Hussein, M. Irmawati, *Catal. Lett.*, 2007, **119(1-2)**, 64; R. Sen, R. Bera, A. Bhattacharjee, P. Gütlich, S. Ghosh, A.K. Murkerjee, S. Koner, *Langmuir*, 2008, **24**, 5970.
17 M.R. Mayura, M. Kumar, A. Arya, *Catal. Commun.*, 2008, **10**, 187; M.R. Maurya, A. Arya, A. Kumar, J.C. Pessoa, *Dalton Trans.*, 2009, 2185; M. R. Maurya, A. Arya, U. Kumar, A. Kumar, F. Avecilla, J.C. Pessoa, *Dalton Trans.*, 2009, 9555.
18 H. Lin, P.A. Maggard, *Inorg. Chem.*, 2008, **47**, 8044; Y. Hu, F. Luo, F. Dong, *Chem. Commun.*, 2011, **47**, 761.
19 R.D. Shanon, C. Calvo, *J. Solid State Chem.*, 1973, **6**, 538.
20 H. Zadrodsky, S. Peles, D. Avnir, *J. Am. Chem. Soc.*, 1992, **114**, 7843; M. Pinsky, D. Avnir, Inorg. Chem., 1998, **37**, 5575.

21 M. Llunel, D. Casanova, J. Cicera, J.M. Bofill, P. Alemany, S. Alvarez, M. Pinsky, D. Yatunir, SHAPE v1.1a "*Program for Continuous Shape Measure Calculations of Polyhedral Xn and MLn fragments*", 2003.
22 S. Alvarez, D. Avnir, M. Llunel, M. Pinsky, *New J. Chem*., 2002, **26**, 996.
23 J. Cicera, P. Alemany, S. Alvarez, *Chem. Eur. J.*, 2004, **10**, 190.
24 "Powder Diffraction File-Inorganic and Organic", ICCD, Pennsylvania. File 38-0252, 2001.
25 "Powder Diffraction File-Inorganic and Organic", ICCD, Pennsylvania. File 86-2248, 2001.
26 "Powder Diffraction File-Inorganic and Organic", ICCD, Pennsylvania. File 22-0454, 2001.
27 "Powder Diffraction File-Inorganic and Organic", ICCD, Pennsylvania. File 73-1032, 2001.
28 "Powder Diffraction File-Inorganic and Organic", ICCD, Pennsylvania. File 29-0945, 2001.
29 "Powder Diffraction File-Inorganic and Organic", ICCD, Pennsylvania. File 45-1054, 2001.
30 J.S. Griffith, The Theory of Transition-Metal Ions, Cambridge University Press, London, 1964.
31 Y. Tanabe, S. Sugano, *J. Phys. Soc. Japan*, 1954, **9**, 753.
32 A.B.P. Lever, *Inorganic Electronic Spectroscopy*, Elsevier Science Publishers B. V., Amsterdam, Nederland, 1984.
33 V. Conte, O. Bortolini, in *The Chemistry of Peroxides Transition Metal Peroxides. Synthesis and Role in Oxidation Reactions*, ed. Z. Rappoport, Wiley Interscience, 2006. and references cited therein; V. Conte, B. Floris , *Inorg. Chim. Acta*, 2010, **363**, 1935.
34 C. Song, *Catal. Today*, 2003, **86**, 211.
35 P. Román, J.M. Gutiérrez-Zorrilla, *J. Chem. Educ.*, 1985, **62**, 167.
36 W.Yingua, *J. Appl. Crystallogr.*, 1987, **20**, 258.
37 A. C. T. North, D.C. Philips, F. S. Mathews, *Acta Crystallogr*., 1968, **A24**, 351.
38 XAREA, Program for X-ray Crystal Data Collection, Stoe, Darmstadt, Germany 2002; Crysalis RED, Oxford Diffraction Ltd. CRYSALIS 1.171.29 version, 2006.
39 G. M. Sheldrick, SHELX97. Programs for Crystal Structure Analysis (Release 97-2). University of Göttingen, Germany, 1997.
40 L. J. Farrugia, *J. Appl. Crystallogr.*, 1999, **32**, 837.
41 T. Hahn, ed., *International Tables for X-ray Crystallography*, Kynoch Press, Birmingham, England, 1974, vol. IV, p. 99.